REVIEW AND STUDY

Monte Carlo Simulation in Surfactant and Polymer Chemistry

by Axel Drefahl
axeleratio@yahoo.com

Published on-line by:
Axel Drefahl in February 2007 in Reno, Nevada (USA)

Originally prepared by:
Axel Drefahl in 1999 at the Technical University
“Bergakademie Freiberg” (University of Mining
and Technology) in Freiberg, Saxony (Germany)

For further information:
E-mail: axeleratio@yahoo.com

Preface

The present review and study was prepared following my presentation at the First Indo-US Workshop on Mathematical Chemistry (January 9-13, 1998) at the Visva-Bharati University in Santiniketan, West Bengal, India (http://www.nrri.umn.edu/India/index.html). This was a very special meeting for me. First of all, I just arrived in time for my presentation, two days later than expected due to thick fog in Dehli. But I was not the only one. I was relieved when I finally made it to Calcutta and boarded the train there to Santiniketan. On the train I ran into fog-delayed late-comers of graph-theoretical fame from Great Britain and Australia and then I knew I was on the right path. Socializing in the warmth and sunshine in the hotel gardens with the other attendees felt surreal after having left the dripping icicles in Freiberg a few days earlier. The final highlight following the workshop was the visit of Agra and the Taj Mahal with some of the workshop participants.

The workshop was a pleasant opportunity to meet old friends and make new ones. I was excited when I received a letter from Prof. R. K. Mohanty suggesting the publication of a monograph on "Some Aspects of Mathematical Chemistry" with broad based articles, introducing different aspects of the subject, primarily for the Indian audience. The present article was furnished accordingly. However, for reasons that were never made completely transparent to me, the monograph never materialized as envisioned. Hence, I decided to publish my contribution independently herein.

In the first place, I want to thank Prof. Subhash C. Basak at the University of Minnesota in Duluth (USA) for inviting me to the First Indo-US Workshop. My thanks also go to Prof. Mohanty for giving the current paper a start.

I also like to thank the *Deutsche Forschungsgemeinschaft* in Bonn (Germany) for its support through the SFB 285/B3 Grant. This special research fund (SFB stands for *Sonderforschungsbereich*) with the title "Particle Interactions in Process Engineering: Fundamentals and Application" included a project on the self-organization of amphiphilic molecules on particle surfaces. The current article is based on my work within that project.

Further, the encouragement and helpful suggestions of Prof. H.-J. Mögel at the Institute of Physical Chemistry at the University of Mining and Technology in Freiberg (Saxony), Uwe Reimer, Olaf Seidel, and Frank Bagusat (then at the same department) and Mirco Wahab at the Chemistry Department of the University in Halle (Saxony-Anhalt) are gratefully acknowledged.

Axel Drefahl
Reno, Nevada
February 2007

Monte Carlo Simulation in Surfactant and Polymer Chemistry

Axel Drefahl
Institute of Physical Chemistry, TU Bergakademie Freiberg,
09599 Freiberg, Germany
E-mail: drefahl@erg.phych.tu-freiberg.de

Abstract

Applications of the Monte Carlo method to selected chemical systems are briefly reviewed. Several models of molecular chains are introduced emphasizing the random walk concept and comparison with scaling predictions. The Monte Carlo approach is illustrated with a system of two interacting, self-assembled monolayers of amphiphile molecules using an off-lattice, good solvent model. Mean size chain properties and density profiles are discussed for separated and interacting layers and compared with results from lattice simulations. It is demonstrated that Monte Carlo simulations compliment both theory and experiment in understanding complex chemical systems and in predicting their properties.

Keywords: Monte Carlo simulation; Molecular conformations; Self-avoiding random walks; Off-lattice models; Scaling predictions; Self-assembled monolayers; Surface-surface interaction

1 Introduction

The Monte Carlo (MC) method is a statistical sampling technique [1, 2]. This method was first used in thermonuclear computations [3] and thereafter has found widespread applications, for example in numerical integration [4–7], image processing [8,9], condensed matter physics [10, 11], and biological modeling [12, 13].

In chemistry alone, MC simulations are today applied to various fields including fluid and crystal science and equation of state (EOS) calculations [14–19], macromolecular and biopolymer chemistry [20–23], sol-gel chemistry [24–28], aggregation kinetics [29–37], surface and interface science [38–41], and quantum chemistry [42–44], just to name a few. General accounts that refresh the required background in statistical mechanics and thermodynamics [45–48] and that supply strategies in the design of efficient MC routines [15, 49, 50] are available. Therein, one also finds all the details to compare the statistical MC approach with the molecular dynamics (MD) simulation techniques. Herein, we confine ourselves to a short review of selected MC applications and a MC illustration with a system of two parallel supported, interacting monolayers.

In the first part of this work we briefly review exemplary chemical systems approached by MC techniques. We start with isolated, flexible homopolymers introducing the random walk and the scaling concept, both playing a central role in theoretical modeling and molecular simulations of surfactant and polymer systems. Then, we summarize models and results from MC simulations for single heteropolymers and multimolecular systems consisting of surfactants or polymers in bulk solution and at interfaces. In the second part we present athermal off-lattice simulations of two interacting monolayers studying monolayer properties as a function of layer penetration.

2 Selected Applications

2.1 Homopolymers

A homopolymer is typically represented as a chain of monomers that are undistinguishable except by their coordinates. Instead of the term monomer, terms such as pearl, bead, sphere, segment, hyperatom, residue or structural unit are found in the literature depending on the considered chain model and application. A particular chain model is specified by the embedding lattice, the type of the bond between pairs of consecutive pearls, the defined type of non-bonding pearl-pearl-interaction, and the chain movement algorithm. Chain molecules have been studied off-lattice, and on two-dimensional (2D) square and triangular lattices [51–54] and on three-dimensional (3D) cubic and tetrahedral lattices [55–66]. Within lattice models, two consecutive pearls in a chain are located on a pair of nearest neighbor (NN) sites and consequently the bond length is fixed by the distance between two NN-sites. This distance is addressed as the lattice constant and often used as the unit length. The number of NN sites for a given lattice site is 4 on the square lattice and 6 on the triangular and cubic lattice. A much higher number of NN sites and some bond flexibility offers the bond fluctuation (BF) model [67] that still has the computational advantages of lattice models. Off-lattice models require numerically more involved algorithms and are computationally expensive, but free of lattice artifacts. Of fundamental interest are the polymer conformational properties [68, 69] that can be calculated by employing MC sampling. The samples are randomly selected conformations generated as random walks (RW). Formalism and application of the random walk concept has been treated elsewhere [70] and a guided tour motivates its implementation for MC sampling [71]. We are primarily interested in chains with non-intersecting pearls.These are modeled as self-avoiding walks (SAW) and the chain model is then said to satisfy excluded volume (EV) conditions. Principal chain properties are defined next, chain models for on-lattice and for off-lattice MC simulations are considered, and scaling is introduced.

2.1.1 Chain definitions and properties

A particular conformation of a chain with N_p pearls is given by the set of the pearl center coordinates $\{\mathbf{r_1}, \mathbf{r_2}, \ldots, \mathbf{r_{N_p}}\}$. The conformation is traced by $N_b = N_p - 1$ bond vectors $\mathbf{b_1}, \mathbf{b_2}, \ldots, \mathbf{b_{N_b}}$ of length l_b, where

$$\mathbf{b_1} = \mathbf{r_2} - \mathbf{r_1}, \mathbf{b_2} = \mathbf{r_3} - \mathbf{r_2}, \ldots, \mathbf{b_{N_b}} = \mathbf{r_{N_p}} - \mathbf{r_{N_{p-1}}}. \tag{1}$$

The sum of these vectors

$$\mathbf{R}_{N_b} = \sum_{i=1}^{N_b} \mathbf{b_i} \tag{2}$$

is called the end-to-end vector of the conformation. Its end-to-end distance R_e equals the scalar length of $\mathbf{R_{N_b}}$. The square of R_e is calculated as

$$R_e^2 = (x_{N_p} - x_1)^2 + (y_{N_p} - y_1)^2 + (z_{N_p} - z_1)^2 \tag{3}$$

where x_1, y_1, z_1 and x_{N_p}, y_{N_p}, z_{N_p} are the coordinates of the two terminal pearls. Each pearl is described by its diameter $d_p \leq l_b$. At this point we consider unconstrained chains with $d_p = 0$ for all pearls. An equilibrium property of a molecular chains is obtained by building the average from a large number of randomly selected, individual conformations. In case of R_e^2, this is the mean-square end-to-end distance [72]

$$\langle R_e^2 \rangle = \langle \mathbf{R}_{N_b} \cdot \mathbf{R}_{N_b} \rangle = \sum_{i,j=1}^{N_b} \langle \mathbf{b_i} \cdot \mathbf{b_j} \rangle = \sum_{i=1}^{N_b} \langle \mathbf{b_i^2} \rangle + 2 \sum_{0<i<j\leq N_b} \langle \mathbf{b_i} \cdot \mathbf{b_j} \rangle \tag{4}$$

Often the dimensionless root-mean-square end-to-end distance, $\langle R_e^2 \rangle^{1/2}/l_b$, is used. Since $\langle \mathbf{b_i^2} \rangle = l_b^2$ for any bond vector, we get

$$\langle R_e^2 \rangle_0 = N_b l_b^2 \tag{5}$$

for the unperturbed state indicated by the subscript 0 next to the right angle. In an unperturbed chain the bond vectors are completely uncorrelated, i.e. $\langle \mathbf{b_i} \cdot \mathbf{b_j} \rangle = \langle \mathbf{b_i} \rangle \cdot \langle \mathbf{b_j} \rangle = 0$ for $i \neq j$. Properties of the unperturbed chain are commonly employed as reference values with which the properties of perturbed chains are compared.

The next property to be introduced is the gyration radius of a conformation [72]

$$R_g^2 = (N_b + 1)^{-2} \sum_{1\leq i<j\leq N_b+1} b_{ij}^2 \tag{6}$$

where b_{ij} is the distance between the centers of pearl i and j. For the unperturbed chain at equilibrium conditions we obtain

$$\langle R_g^2 \rangle_0 = (N_b + 1)^{-2} \sum_{1\leq i<j\leq N_b+1} \langle b_{ij}^2 \rangle_0 \tag{7}$$

where $\langle b_{ij} \rangle_0$ is the mean distance between the centers of pearl i and j. $\langle b_{ij} \rangle_0$ may be considered as the mean-square end-to-end distance of a chain with $(j - i)$ bonds.

Thus, with (5) we have $\langle b_{ij}\rangle_0 = (j-i)l_b^2$ and with (7) we get

$$\langle R_g^2\rangle_0 = (N_b+1)^{-2} l_b^2 \sum_{1\le i<j\le N_b+1} (j-i) \tag{8}$$

Replacement of $(j-i)$ by k leads to

$$\langle R_g^2\rangle_0 = (N_b+1)^{-2} l_b^2 \sum_{j=1}^{N_b}\sum_{k=1}^{j} k = (N_b+1)^{-2} l_b^2 \sum_{j=1}^{N_b} j(j+1)/2 \tag{9}$$

With $\sum_{j=1}^{N_b} j = \frac{1}{2}N_b(N_b+1)$ and $\sum_{j=1}^{N_b} j^2 = \frac{1}{6}N_b(N_b+1)(2N_b+1)$ we finally obtain

$$\langle R_g^2\rangle_0 = \frac{1}{6} l_b^2 \frac{N_b(N_b+2)}{N_b+1} \tag{10}$$

With (5) and (10) we get the ratio

$$\frac{\langle R_e^2\rangle_0}{\langle R_g^2\rangle_0} = 6\frac{N_b+1}{N_b+2} \tag{11}$$

and in the limit $N_b = \infty$

$$\frac{\langle R_e^2\rangle_0}{\langle R_g^2\rangle_0} = 6,\ N_b \to \infty \tag{12}$$

Equations (1) to (4) and (6) apply in general whereas the remaining equations apply to unperturbed off-lattice chains in which all bonds are of the same length l_b. Additional properties are defined elsewhere [73].

2.1.2 On-lattice chain models

Starting with the first and second pearl placed onto NN lattice sites $\mathbf{r_1}$ and $\mathbf{r_2}$, respectively, a chain is grown by consecutively appending new pearls to the current chain until a chain with N_p pearls is obtained. During growth, the site for the new pearl is drawn from a set, S_{NN}, of k_{NN} NN sites depending on the selected lattice type and on the growth algorithm, where k_{NN} is the coordination number of the lattice, i. e. the lattice constant. The lattice spacing length is l_b. On a square lattice, for example, the lattice site of the second pearl in the chain, $\mathbf{r_2} = (x_2, y_2)$, has the $k_{NN} = 4$ NN-sites $\mathbf{r_{NN1}} = (x_2 + l_b, y_2)$,

$\mathbf{r_{NN2}} = (x_2 - l_b, y_2)$, $\mathbf{r_{NN3}} = (x_2, y_2 + l_b)$, and $\mathbf{r_{NN4}} = (x_2, y_2 - l_b)$. But one of these sites is already occupied by the first pearl and has to be excluded to satisfy the EV condition. The growth algorithm determines which of the three remaining NN sites are allowed to be chosen. Let us assume here that $\mathbf{r_1} = \mathbf{r_{NN1}}$. Then, the two-choice 90° growth algorithm allows to choose between sites $\mathbf{r_{NN3}}$ and $\mathbf{r_{NN4}}$, whereas the three-choice 90° growth algorithm allows to choose from all of the three remaining NN sites. The two-choice 120° and the five-choice 60° growth algorithm for the triangular lattice are defined in the same manner [52]. Similar algorithms have been established for chain growth on three- and four-dimensional lattices [55, 74]. Within any of these growth algorithms NN sites are chosen randomly with equal probability to generate a particular chain conformation. While the chain is growing there is a good chance that the chosen NN site is already occupied by a previous pearl. In such a case chain growth has to be terminated to guarantee unbiased sampling of SAW conformations. The inefficiency in sampling long chains ($N_p > 100$) is known as the attrition problem [71]. The attrition strength can be quantified and depends on the selected lattice chain model [52, 55, 75].

Attrition is avoided by employing biased sampling in which the subset $\mathbf{V}_{NN}$ of vacant NN sites is extracted from $\mathbf{S}_{NN}$. After this preselection a vacant NN site is randomly and with equal weight chosen from $\mathbf{V}_{NN}$. However, completed conformations are now generated with different weights. Rosenbluth and Rosenbluth [51] have developed a weighting scheme that counts all successfully generated chains equally as required for statistical properties of equilibrium chains. For the square lattice, the Rosenbluth-Rosenbluth-weight is calculated as

$$W_{RR} = \frac{1}{4 \cdot 3^{N_b - 1}} \prod_{i=1}^{N_b} |\mathbf{V}_{NN,i}| \tag{13}$$

where $\mathbf{V}_{NN,i}$ is the set of vacant NN sites of the i-th pearl. W_{RR} for other lattice types is calculated accordingly by only adjusting the prefactor. The average values of the SAW properties $\langle P \rangle$ with, say, $P = R_e^2$ or R_g^2 are estimated by a ratio of weighted averages [73]:

$$\langle P \rangle \approx \frac{\sum_{j=1}^{N_{samp}} W_{RR,j} P_j}{\sum_{j=1}^{N_{samp}} W_{RR,j}} = \frac{\sum_{j=1}^{N_{samp}} (\prod_{i=1}^{N_b} |\mathbf{V}_{nn,i}|)_j P_j}{\sum_{j=1}^{N_{samp}} (\prod_{i=1}^{N_b} |\mathbf{V}_{nn,i}|)_j} \tag{14}$$

where each summation is done over all N_{samp} completely generated SAWs. This kind of MC sampling that includes previewed self-avoidance along with weight calculation is called inversely restricted sampling (IRS) [73]. The IRS method is widely used for the generation of small surfactant chains, but still leads to growth termination for longer chains in which self-trapping, i.e. $|\mathrm{V}_{nn,i}| = 0$, occurs for large i. On average, for example, a three-choice $90°$ SAW on the square lattice lasts only 71 steps [76]. That is why there is no best choice of a growth algorithm and one often needs to design a modified or novel algorithm depending on the problem at hand.

2.1.3 Off-lattice chain models

The first step towards off-lattice simulation is taken with the BF model. This model is still based on a square or a cubic lattice, but monomers occupy a 2×2-square or a $2 \times 2 \times 2$-cube of lattice points, respectively. Pairs of NN-sites are flexibly defined by a set of different bond vectors allowing for discrete bond angles and bond lengths [67].

The freely jointed (FJ) and the freely rotating (FR) chain are off-lattice models with fixed bond length but with angle flexibility. FJ chains have arbitrary bond angles between $0°$ and $180°$ and arbitrary bond rotation angles between $0°$ and $360°$, whereas in FR chains the bond angle Θ is fixed [68, 72]. The bond rotation angle ϕ_i of bond i measures the dihedral angle between two planes defined by bond pairs ($\mathbf{b_{i-1}}$,$\mathbf{b_i}$) and ($\mathbf{b_i}$,$\mathbf{b_{i+1}}$), respectively. The FJ chain is exactly mathematically treatable and was introduced as a polymer chain model by Kuhn [77]. FJ chains are unperturbed and modeled with equations (1) to (12). FR chains are restricted by the fixation of the bond angle with consequences to their mean size properties. Equation (5), for example, has to be modified by additional terms [68] to

$$\langle R_e^2 \rangle = N_b l_b^2 + 2 N_b l_b^2 x \left(\frac{1 - x^N}{1 - x} \right) - 2 l_b^2 x \left(\frac{1 - x^N}{(1 - x)^2} - \frac{N x^N}{1 - x} \right) \tag{15}$$

where $x = \cos\Theta$. As $N_b \to \infty$, this equation approaches

$$\langle R_e^2 \rangle = N_b l_b^2 \left(\frac{1 + x}{1 - x} \right) \tag{16}$$

Further restrictions to the conformational freedom is introduced by various potential interaction terms that apply between pairs of monomers.

Interaction between non-bonded monomers is modeled either by non-intersecting hard pearls with a given radius or by soft pearls for which a potential scheme of pairwise interaction is applied. Hard pearl chains are also addressed as pearl-necklace chains. The model of a FR pearl-necklace chain allows the selection of ϕ_i freely as long as the pearls do not overlap. Other off-lattice models are based on dynamically changing bond lengths. The bead-spring chain that models the bonds as harmonic oscillators is just one example. Model potentials including bond length and bond angle vibrations along the molecular backbone have been employed to model single polyethylene chains [78]. Various algorithms have been established to grow or to move both on- and off-lattice chains depending on the simulation goal [22, 79].

2.1.4 Scaling concepts

MC simulations are typically applied to coarse-grained models neglecting atomistic details. Nevertheless, the observed behavior and critical phenomena of chemical systems are often correctly predicted in terms of simple scaling laws [80, 81]. For polymer systems the asymptotic behavior of a property P is expressed by

$$P = a_s N_p^{2\nu}, \quad \text{as } N_p \to \infty, \tag{17}$$

where a_s is the scaling factor and ν is the universal exponent. The latter is the same for systems associated with the same universality class. For a given class of systems structural and energetic details are irrelevant for universal scaling. Only the nonuniversal scale factor has to be adjusted to specific details. For P being a squared global dimension like the squared end-to-end distance or the squared radius of gyration of an isolated chain with $N_p \to \infty$, (17) turns into the scaling relation [71, 82]

$$P = \langle l_b^2 \rangle N_p^{2\nu} \quad \text{with} \begin{cases} \nu \approx 0.59 & : \quad T > T_\Theta \\ \nu \approx 1/2 & : \quad T = T_\Theta \\ \nu \approx 1/3 & : \quad T < T_\Theta \end{cases} \tag{18}$$

where T is the system temperature and T_Θ is the Θ-temperature defined by [83]

$$\lim_{N_p \to \infty} \left. \frac{\langle R_e^2 \rangle}{N_p} \right|_{T=T_\Theta} = \text{const.} \tag{19}$$

Θ-conditions describe the state at which an isolated polymer chain behaves as a random coil completeley neglecting any intramolecular interactions. However, T_Θ has also been defined as the point at which the second virial coefficient of a polymer solution vanishes [83]. For the class of good solvents ν is above, and for the class of poor solvents ν is below the Θ-condition value $1/2$. Considering an isolated polymer chain in solution, this can be in the extended coil state ($T > T_\Theta$), the random coil state ($T = T_\Theta$), or the dense globular state ($T < T_\Theta$). Mean size properties of the polymer at the random coil state scale with $\nu = 1/2$ just as the self-intersecting RW properties do; however, the local properties of a Θ-chain differ from the local RW properties [83]. Simulations are said to be athermal when a SAW model solely with EV interactions ($T = \infty$) is employed. Since $T = \infty > T_\Theta$, athermal simulations always investigate good solvent conditions and an athermal solvent is said to be a very good solvent. Applications of scaling relations to viscosity and light scattering behavoir of dilute polymer solutions that correlate with mean size properties of the molecular chain are discussed in the literature [77, 84, 85].

2.2 Branched Polymers

A branched polymer is a special case of a tethered polymer chain system in which one chain end or both ends are attached to a d dimensional surface [86]. A branched polymer is either a many-arm star polymer ($d = 0$) or a comb polymer ($d = 1$). In a star polymer one end of each chain is attached to a small central core to form a single molecule. In a comb polymer one end of each chain is attached to a backbone chain. The case of a polymer brush ($d = 2$), in which each chain is grafted to a flat surface, is considered later. The random walk concept is easily extended to sample branched chains and MC simulation has been applied to star polymers [87–94] and to comb polymers [95, 96].

A uniform f-arm star polymer has f unbranched arms each having the same number of pearls, $N_{p,f}$. Note that a linear polymer chain is a 2-arm star molecule. Exact and MC calculations show that the mean square end-to-end distance of an arm, $\langle R_e^2(f)\rangle$, increases with f [87]. Theoretical treatment leads to the relation

$$\langle R_e^2(f)\rangle = A(f) N_{p,f}^{2\nu(f)}, \quad \text{as } N_{p,f} \to \infty, \tag{20}$$

where $A(f)$ is an increasing function of f and $\nu(f) = \nu$ is independent of f. Hence, $A(f_2)/A(f_1) > 1$ should apply if $f_2 > f_1$ and for the ratio $A(4)/A(3)$ the value 1.056 was theoretically predicted for the 3D case and the values 1.05 ± 0.01 and 1.04 ± 0.02 were found by simulation on the simple cubic and the tetrahedral lattice, respectively, demonstrating that the ratio is universal, i. e. lattice independent [87]. Theoretical treatments also predict that the mean square radius of gyration, $\langle R_g^2\rangle$, for a uniform f-star is independent of f and scales with the exponent 2ν of the linear chain as $N_{p,f} \to \infty$ [87]. Formal replacement of the unbranched arms of star polymers by branched, tree-like structures leads to dendrimers, which have been modeled by off-lattice MC simulations to evaluate the scaling behavior [94]. The ultimate properties of dendrimers, however, depend largely on the functional groups at the chain ends [97].

An example for the MC analysis of comb polymers is the study of the equilibrium conformations of combs with a flexible backbone and flexible side chains grafted at regular separations onto the backbone [95]. Using the BF model, the global and local comb conformational structure and the gyration radius was discussed as a function of side chain and spacer length and reasonable agreement with scaling predictions was found.

2.3 Biopolymers

Biopolymers are heteropolymers. In contrast to the study of homopolymers where MC simulations are used for averaging conformations, biopolymer simulations including exhaustive and MC methods are often devoted to find specific conformations corresponding to a biologically significant, folded state [98–101], to a state preorganized for intrachain loop formation [102, 103] and to states modeling protein-surface interaction [104, 105]. A simple lattice model has been developed that builds protein chains simply from either hydrophobic (H) or hydrophilic (P) monomers representing amino acids [104, 106]. An energy scheme has been defined for the three interactions HH, HP, and PP of non-bonded monomers on adjacent lattice sites. The goal is to find the native state, which is the state of lowest energy state, for a given sequence. Using 2D lattice models, the native state of short sequences can be determined by exhaustive enumeration, whereas MC simulation is suitable to obtain the native state and closely related states of long sequences [100, 107]. Related states such as denatured but still compact states are of interest as the intermediate states in the folding pathway [106]. Moving on to 3D off-lattice simulations, the same protein model of merely two monomer types is sufficient to follow the gradual compactification of chains depending on their sequence and on the system temperature [108]. MC methods for the evaluation of local conformations in polypeptide chains have been integrated into a hierarchic procedure to predict protein folding (LINUS) [106]. The interested reader is referred to a recent work that demonstrates the application of lattice MC dynamics to a protein with 125 monomers and that provides further references to literature on the very subject [101].

2.4 Polymer Solutions and Mixtures

Scaling relation (18) refers to polymers in infinitely dilute solutions wherein the chains form isolated, random coils. Increasing the polymer concentration in very good solvents, the coils eventually start to overlap and the solution arrives at the semidilute regime. At the transition concentration the coils begin to be densely packed [109] and the bulk monomer concentration aproaches the monomer concentration inside the coils. In semidilute solutions the monomer concentration becomes independent of N_p and thus thermodynamic properties depend on the concentration but not on N_p. Considering the complete range of monomer concentrations, mean size global and local chain properties in good and Θ solvent have thoroughly been studied by MC-simulation on a cubic lattice [82]. Typically, simulation data are discussed by comparison with results from liquid lattice theory. This theory provides a framework to approximate thermodynamic properties of polymer solutions employing mean-field methods [110]. Based on the Flory-Huggins (FH) lattice model, polymer solutions and mixtures have been studied by MC simulations [111–119] as an independent technique to check the validity of mean-field approximations.

Successful MC-simulations with the FH-model must use the grand-canonical ensemble [112], for which the chemical potential differences are fixed instead of the number of molecules in the system. In a binary solution of polymers A and B in a given solvent, grand-canonical MC-simulations (GCMC) can be performed by simply transforming A chains into B chains and vice versa. This transformation move has to be applied in addition to the usual chain moves such as flip, kink, and crankshaft moves. Sampling of the fluctuations of the order parameter, $\langle|(N_B - N_A)/(N_B + N_A)|\rangle$, where N_A and N_B are the number of molecules of A and B, respectively, a collective structure factor, S_{coll}, is obtained as a function of the order parameter and the fixed model parameters [112]. This quantity has experimental relevance since it is accessible from small angle light, x-ray, and neutron scattering.

2.5 Self-Assembled Surfactants

Surfactants in solution are known to form self-assembled structures such as micelles, vesicles and bilayers if the surfactant structure and the solution properties meet apropriate conditions. Characteristic properties of micelle systems are the micellar aggregation number and the critical micelle concentration (cmc) [120–123], for which predictive methods based on quantitative structure-property relationships (QSPR) [124, 125] and on theoretical approaches [126] exist. These approaches are typically limited in predicting the dynamic behavior of the aggregate size, shape and interface, especially for more complex systems including host molecules, whereas MC-simulation allow to mimic experiments on such coopera-

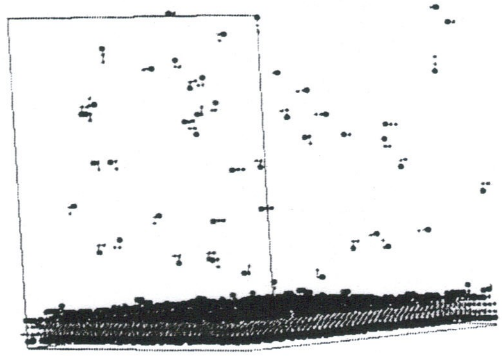

Figure 1: Self-assembly of amphiphiles into a bilayer at an impenetrable surface (Courtesy of Uwe Reimer).

tive self-assembly processes. With increasing computer resources, studies of self-assembly will become less restricted allowing for more sophisticated models that incorporate detailed atomistic geometries and interactions. Current MC simulations, however, rely on simplified models that emphasize universality and capture the essential physics by coarse-graining.

Micelles. Mean size and shape parameters of micelles, pearl distribution, and cluster size distribution have been studied in lattice MC calculations for short diblock copolymers, $A_m B_n$ with $m, n \leq 16$, in bulk solution [127–135], on a single surface [136] and between two planar surfaces [137]. Similarly, bulk solutions have been investigated by including additional solutes to obtain the locus of solubilization and the micelle-solvent partition coefficient of the solute [138]. The latter MC study further shows that solute addition decreases the cmc and increases the micellar size and that the partition coefficient is independent of the surfactant concentration but increases with solute concentration. Off-lattice MC simulations have been employed to 2D multimicellar systems studying regular and inverted micelles for both neutral and ionic surfactants [139].

Vesicles and Bilayers. Phase transition behavior and the change of cluster size distribution as a function of surfactant concentration and system temperature has been analyzed with cubic lattice simulations in the NVT ensemble for flexible amphiphiles with tail-solvent, head-solvent, and head-head interaction [140]. In cubic lattice simulations with one- and two-tail amphiphiles self-organization into vesicles has been observed and vesicle stability, density profiles and aggregation dynamics were discussed [141]. Cubic lattice simulations with three-segment and bolaform six-segment flexible amphiphiles in the NVT ensemble with a constant water content of 90% have resulted into the formation of layer structures at low temperatures by merely applying repulsive NN interactions between alike monomers [142, 143]. A sharp phase transition towards higher temperatures occurs for both types of surfactants indicated by a significant peak in plots of the heat capacity *vs.* temperature. Further, mixtures of both surfactant types [143] and self-assembled layer structures on solid surfaces [144] have also been studied by MC simulation. Figure 1 illustrates the self-assembly of 3-segment amphiphilic molecules (one hydophilic head segment, two hydrophobic tails segments) into a bilayer at an hydrophilic, impenetrable, planar surface based on a cubic lattice MC simulation in the NVT ensemble. Empty lattice sites represent the water-like solvent. The ordered crystalline-like bilayer state of Figure 1 undergoes at higher temperature a transition into a liquid-like, less ordered layer phase of lower density and with further temperature increase the layer disappears. Phase transitions have been detected by plotting the heat capacity and the orientation order parameter against the temperature.

2.6 Supported Monolayers

Self-assembly not only occurs in bulk solutions but also at interfaces (Figure 1). MC simulations are use to study the surface deposition processes [145], adsorption equilibria [146–151], and the structural properties and the phase behavior of monolayers [75, 152–173]. The investigated monolayer properties are for example mean size molecular properties, tilt behavior, ordering parameters, and density profiles. Long, flexible, grafted chains are modeled as polymer brushes for which consistent scaling relations are obtained using both on- and off-lattice simulations [86]. For high-density surfactant layers the use of off-lattice models has been recommended since lattice artefacts where found in a systematic study of several lattice types [174].

In the following illustration of a MC study we consider supported monolayers of FR-chains grafted onto two planar, parallel surfaces. The two equally dense monolayers face each other and will interact depending on the variable distance between the surfaces. We demonstrate how to construct the model and test its implementation and we compare simulation results with those obtained with lattice models.

3 Interacting Monolayers

3.1 Off-Lattice Model

System. In our off-lattice model we consider two parallel surfaces $\mathrm{S_I}$ and $\mathrm{S_{II}}$ that are separated by a distance d_S. Both surfaces are planar and impenetrable and support grafting of amphiphilic chain molecules. The system is bounded by a cuboid of size $L_x L_y L_z$, where $L_x = L_y$ and $L_z \geq d_S$. Periodic boundary conditions apply in $x-$ and $y-$direction, whereas the z-direction is confined by $\mathrm{S_I}$ at $z = 0$ and by $\mathrm{S_{II}}$ at $z = d_S$. The model implementation is based on the cell index method that divides the cuboid into a regular lattice of cells [15]. This method enables efficient screening of molecular neighborhoods, but does not imply any discretization to our model.

Chain model. The off-lattice chains are defined and characterized by (1) to (4 and (6). We use the FR chain model of the pearl-necklace type in which the N_p pearls of the chain are treated as hard spheres. The pearls have the same diameter d_p and different centers $\mathrm{C_i}= (x_i, y_i, z_i)$ where $1 \leq i \leq N_p$. Consecutive pearls are connected by a bond of length $l_b \geq d_p$. Pearl-pearl and pearl-surface overlaps are forbidden to satisfy the EV condition. Each FR chain represents an amphiphilic molecule of one head pearl ($i = 1$) and $N_p - 1$ tail pearls ($1 < i \leq N_p$). A chain is grafted onto $\mathrm{S_I}$ and $\mathrm{S_{II}}$ so that the z-component of $\mathrm{C_1}$ is either $z_1 = d_p/2$ and $z_1 = d_S - d_p/2$, respectively. The number of chains grafted onto $\mathrm{S_I}$ and $\mathrm{S_{II}}$ are $N_{ch,I}$ and $N_{ch,II}$, respectively, and in this study $N_{ch} = N_{ch,\mathrm{I}} = N_{ch,\mathrm{II}}$ applies.

Sampling of conformations. The second pearl is positioned at C_2 so that the straight line C_1C_2 is perpendicular to the surface plane and the distance between C_1 and C_2 is $|\mathbf{b_1}| = l_b$. The position for the center of the third pearl is determined by the bond vector $\mathbf{b_2}$, which has to be appended to the current chain at C_2. The compliment of the angle between $\mathbf{b_1}$ and $\mathbf{b_2}$ is the bond angle Θ which is fixed whereas the bond rotation angle φ can freely be chosen from values between 0 and 2π. In other words, a position for the third pearl can be chosen from any point on the circle obtained by rotating $\mathbf{b_2}$ around C_1C_2. Here, we apply uniform discretization (UD) [175] to the bond rotation angle. Instead of an infinite number of trial positions we restrict our choice to the set S_{UD} with $N_{UD} = |S_{UD}|$ trial positions that are given by $\phi = 0, 2\pi/N_{UD}, \ldots, 2\pi(N_{UD} - 1)/N_{UD}$. Trial positions that would lead to overlap are rejected and the choice of a position is done with the remaining set of equally probable positions, V_{UD}, from which one position is randomly selected as the actual center of the third pearl. We repeat this procedure for every of the following pearls to complete the FR chain. This algorithm is analogous to the aforementioned IRS algorithm to sample conformations of lattice chains. Instead of the lattice constant there, our algorithm is characterized by the degree of discretization N_{UD}. As $N_{UD} \to \infty$, we approach real off-lattice simulation. The selection of reasonable values for N_{UD} has to be guided by the need for off-lattice reality against the cost of computation time. In analogy to the Rosenbluth-Rosenbluth-weight in (13), we calculate the weight for the conformation of a grafted FR chains as

$$W_{UD} = N_{UD}^{1-N_b} \prod_{i=2}^{N_b} |\mathbf{V}_{UD,i}| \tag{21}$$

During MC simulation, attempts are made to replace the current conformation of a randomly selected chain by a trial conformations. Assuming the weights of the current and the trial conformations to be W_{UD}^{cur} and W_{UD}^{try}, respectively, then the trial chain is accepted if either $W_{UD}^{cur} \leq W_{UD}^{try}$ or, in the case that $W_{UD}^{cur} > W_{UD}^{try}$, the trial conformation is accepted with probability $P_{acc} = W_{UD}^{try}/W_{UD}^{cur}$.

Mean size properties. Mean size properties of the chains are estimated in analogy

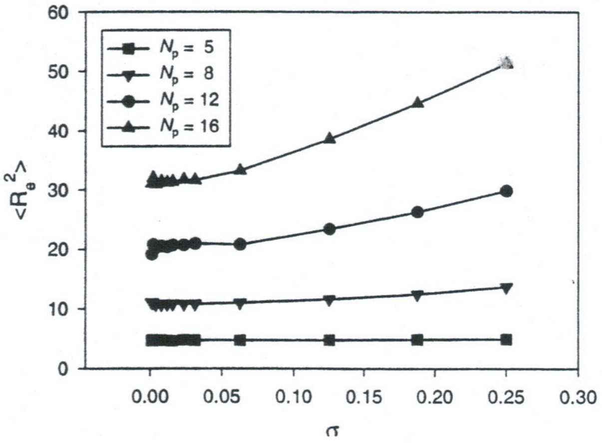

Figure 2: Mean-square end-to-end distances as a function of surface coverage for four different chain lengths.

to (14) by a ratio of weighted averages:

$$\langle P\rangle \approx \frac{\sum_{j=1}^{N_{samp}} W_{UD,j} P_j}{\sum_{j=1}^{N_{samp}} W_{UD,j}} = \frac{\sum_{j=1}^{N_{samp}} (\prod_{i=2}^{N_b} |\mathrm{V}_{UD,i}|)_j P_j}{\sum_{j=1}^{N_{samp}} (\prod_{i=2}^{N_b} |\mathrm{V}_{UD,i}|)_j} \tag{22}$$

where now N_{samp} refers to the number of replicas sampled from all of the generated ensemble configurations. More details are provided further below in the simulation description. For the sake of readability we have included just one individual chain into the summation, but to define mean monolayer properties we have to included all chains grafted onto the same surface.

Layer properties. We are interest in pearl density distributions. We define $p_e(z)$ as the probability to find the free end pearl in a layer between z and $z + dz$ from surface S1. We calculate replica-averaged probabilities

$$p_e(z) = \frac{1}{N_{rep}} \sum_{r=1}^{N_{rep}} \frac{N_{e,r}(z, z+dz)}{N_{ch}} \tag{23}$$

where $N_{e,r}(z, z + dz)$ is the number of end pearls in the r-th replica with their center between the planes at z and $z + dz$. The number of replicas is N_{rep}.

Density profiles are derived from a sequence of plane densities Φ at equidistant z

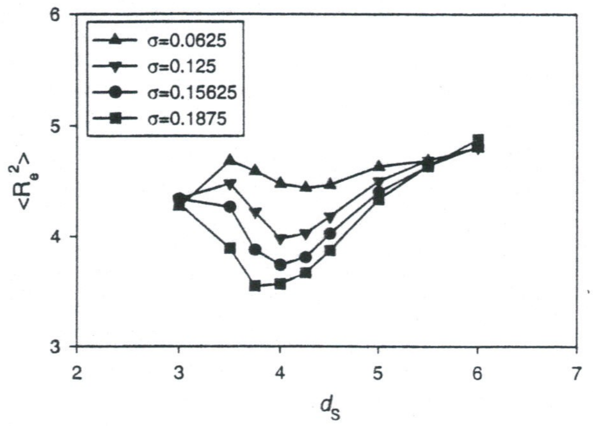

Figure 3: Mean-square end-to-end distances as a function of the surface-surface distance for four different surface coverages.

values as

$$\Phi_d(z) = \frac{1}{N_{rep}} \sum_{r=1}^{N_{rep}} \sum_{s=1}^{N_{r,c}(z)} r_{r,s}^2(z) \tag{24}$$

where $N_{r,c}(z)$ is the number of pearls that are cut in the r-th replica by a surface-parallel plane at z. The circle obtained by such a cut with the s-th pearl has radius $r_{r,s}(z)$.

Simulations. Particular simulations were performed within the NVT-ensemble with a constant number of molecular chains, $N = 2N_{ch}$, a constant volume, $V = L_x L_y L_z$, and a constant temperature, $T = \infty$ (athermal simulations). A particular configuration of the simulated system, in which each chain exhibits a temporary conformation, is said to be a replica of the ensemble. Each simulation run began with an ordered, overlap-free start configuration that was equilibrated in subsequent MC-steps. During a MC-step, a trial was made to regrow each chain at a different location with a new conformation. The new location was randomly selected through a head pearl jump over a distance $d_j \leq L_x/2$, allowing for both the quenched and the annealed case known for the lattice model [159]. In the

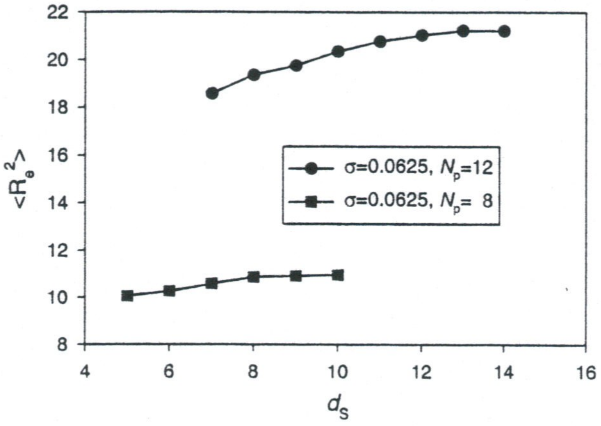

Figure 4: Mean-square end-to-end distances as a function of the surface-surface distance for two different chain lengths. The surface coverage is equal to that of the first curve in Figure 3.

quenched case ($d_j = 0$) the grafting sites are fixed, whereas in the annealed case ($d_j > 0$) the grafted heads diffuse laterally. First, we applied about 10^3 MC-steps to shake the system, i. e. to generate random chain conformations accepting every new conformation that obeyed the EV-condition. Then, we equilibrated the system by accepting weighed trial conformations due to the aforementioned criterium. We applied at least $2.5 \cdot 10^5$ equilabration MC-steps, although we could show with selected runs that fewer MC-step are sufficient to arrive at the equilibrated state. The equilibration process was monitored by observing the change of selected mean size properties. During production the fluctuations in the equilibrated state were simulated. We saved production replicas at regular intervals. At least 10^4 MC-steps were performed for production. Resulting properties were all obtained as averages over the replicas.

A number of simulations were performed to test the algorithmic behavior and we continue by reporting the corresponding results. Then, simulations were run to systematically study the structure of the two monolayers by varing d_S. We distinguish between three different states of monolayer-monolayer interaction. In the separation state, d_S is greater than the maximum height that can be gained by the end pearls so that any interaction between chains from opposite layers is excluded. If d_S is small enough for the end pearls to be able to contact the opposite surface, we speak of the bridging state. The in-between-state is called the penetration state. We performed simulations for all three states with a surface coverage, $\sigma = N_{ch}/L_x L_y$, up to 0.25 on each surface. All simulations used the chain parameters $d_p = l_b = 1$ and $\Theta = 90°$. The chain length was varied between 5 and 16 pearls.

3.2 Results and Discussion

Assessing Performance. Before producing modeling results we have to convince ourselves that the implemented algorithms perform properly. Since conformation sampling is at the core of our simulations we have in detail verified the chain growth algorithm. In particular, we have studied its performance in relation to the UD of the bond rotation angle. This was done for non-grafted chains in an unbounded system with $d_S = \infty$. Over 12 runs we have changed N_{UD} from 4 and 64. In each run 10^6 conformations of FR-chains, always with $N_p = 16$ pearls were sampled to calculate $\langle R_e^2 \rangle$. We obtained a mean value of 15.003 ± 0.0131 for $\langle R_e^2 \rangle$, which is in excellent agreement with the calculated value of 15 using (15) with $\Theta = 90°$. Further, we would expect a linear correlation between the sampling time and N_{UD} and the regression equation

$$t/t_4 = (0.1369 \pm 0.01672) + (0.2186 \pm 0.00046) N_{UD} \qquad (25)$$

with a correlation coefficient of 0.99998, where t_4 is the sampling time needed in the run with $N_{UD} = 4$, confirms our expectation. The largest absolute deviation between theoretical and simulated $\langle R_e^2 \rangle$ was 0.042 obtained for the run with $N_{UD} = 4$, whereas runs with higher N_{UD} exhibited smaller deviations but required more computation time. Including further pre-studies we found $N_{UD} = 8$ to be an agreeable compromise and all the following simulations use this setting.

Layer characterization. We found the relations $\langle R_e^2 \rangle_I = \langle R_e^2 \rangle_{II}$ and $\langle R_g^2 \rangle_I = \langle R_g^2 \rangle_{II}$ to be fulfilled with very good accuracy for various interaction states. These

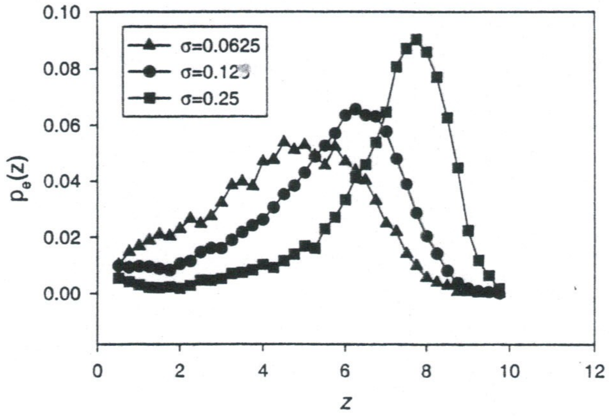

Figure 5: Free end-pearl probabilities as a function of the distance from the grafting surface for three different surface coverages.

equalities come with no surprise since we exclusively studied systems with $N_{ch,I} = N_{ch,II}$ and $N_{p,I} = N_{p,II}$. Therefore, we simplify our following discussion by considering $\langle R_e^2 \rangle = \langle R_e^2 \rangle_I$ and $\langle R_g^2 \rangle = \langle R_g^2 \rangle_I$. Figure 2 shows $\langle R_e^2 \rangle$ as a function of the surface coverage ($0 < \sigma \leq 0.25$) for four different chain lengths in the separation state. For the case $N_p = 5$ we see that $\langle R_e^2 \rangle$ is almost constant whereas for longer chain length $\langle R_e^2 \rangle$ monotonously increases with increasing surface coverage. We found the same behavior for $\langle R_g^2 \rangle$. Comparable results have been obtained with lattice MC simulations of amphiphile monolayers on planar [165] and on nanorough [142] surfaces. If we think of the arm number f in star polymers as the coverage of the surface core, we find the same behavior there: the mean size properties of arms in star polymers increase with increasing number of arms, i. e. increasing number of coverage (compare with (20) and discussions in [86]). The overall picture is that an increase in the density of grafted chains results into more and more elongated chains with mean size properties that are larger than those for the coil-like conformation of the isolated chains at low densities. Now we report results for interacting monolayers. Beginning with very short chains ($N_p = 5$), we have studied all three interaction states up to a surface coverage of 0.1875. The

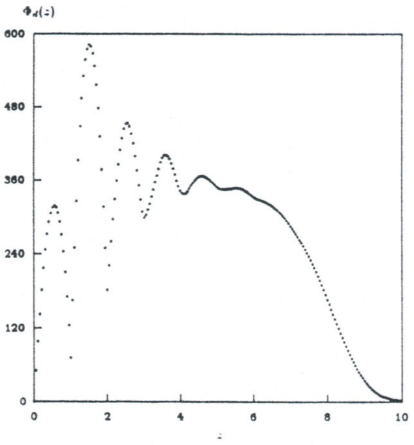

Figure 6: Density profile of a monolayer of 16-mers with $\sigma = 0.25$.

dependencies of $\langle R_e^2 \rangle$ on d_S are displayed in Figure 3. For the separation state ($d_S > 5.5$) we observe that $\langle R_e^2 \rangle$ is independent of σ in concordance with the results from Figure 2. For the bridging state $\langle R_e^2 \rangle$ is again independent of σ, but with a value of $\langle R_e^2 \rangle$ lower than that at the separation state.

Most striking, in the penetration state of Figure 3 $\langle R_e^2 \rangle$ decreases with increasing surface coverage irrespective of d_S. This finding is opposite to the above discussed overall picture of chain elongation with increasing density. One may explain this effect by the entropic repulsion of the two opposed monolayers. The probability of elongated chains descreases as the opposite layer is getting more densely packed.

Further, around $d_S = 4$ a minimum occurs for each curve in Figure 3 and $\langle R_e^2 \rangle$ increases as the bridging state is approached for a given surface coverage. At the beginning of the bridging state the two layers are completely merged and the pearl density has doubled. One may speculate that elongated chains are getting more likely at this state of much higher density since they would allow closer packing, for example, into configurations in which opposite chains could be arranged by

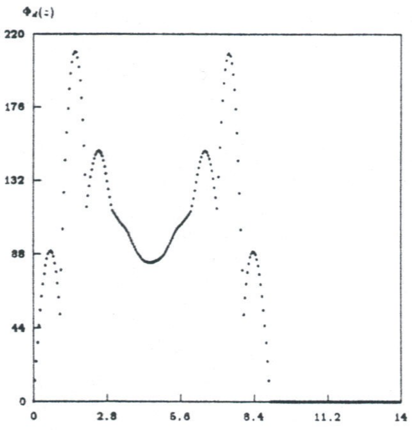

Figure 7: Density profile of two interacting ($d_S = 9$) monolayers of 12-mers with $\sigma = 0.0625$.

interdigitation.

The results for longer chains ($N_p = 8$ and n_p=12) for $\sigma = 0.0625$ are shown in Figure 4. Clearly, $\langle R_e^2 \rangle$ is decreasing with increasing pearl density (i. e. decreasing d_S) just as we have found for $N_p = 5$. However, for the longer chains no $\langle R_e^2 \rangle$ minimum occurs in the penetration state. Comparison with Figure 3 shows that the minimum is only weakly pronounced for $\sigma = 0.0625$ and a further discussion of the minimum has to wait for simulation results of penetrating layers with higher surface coverage not available in the current work.

Figure 5 depicts the distribution of the free end pearls for three different surface coverages of chains with $N_p = 16$. Broad distribution of the end pearls similar to results from lattice polymer brush simulations ($N_p = 30$) [159] are found. Our results also agree with the lattice simulation results in that, as $z \to 0$, the end pearl densities stay nonzero contradicting self-consistent field predictions [159].

Figure 6 illustrates a typical density profile of grafted chains ($N_p = 16, \sigma = 0.25$).

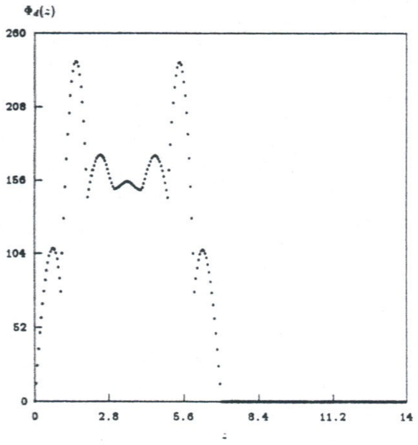

Figure 8: Density profile of two interacting ($d_S = 7$) monolayers of 12-mers with $\sigma = 0.0625$.

Similar density profiles have been found with lattice simulations and self-consistent field calculations [158,159,165,173]. A density maximum occurs near the grafting surface and the density then falls off smoothly to zero. Here, the special geometry at the grafting site and the hard sphere geometry leads to pronounced density oscillations, which, less pronounced, have already been observed in density profiles obtained with the BF model. The oscillations level off after a few bond lengths away from the surface. We also obtained density profiles for interacting monolayers ($N_p = 12, \sigma = 0.0625$). Near the separation state two distinct, oppositely faced profiles, each very similar to the profile of Figure 6, appear. Further interpenetration leads to profiles similar to the one shown in Figure 7 ($d_S = 9$). Density maxima obscured by density oscillations can be seen on both sides near the grafting surface. A local density minimum is observed halfway between both surfaces. Our profiles for $d_S > 7$ look similar to the weak overlap regime profiles that were found in MC simulations of telechelic chains grafted as loops onto the same and as bridges onto both surfaces [176]. For the strong overlap regime ($d_S = 7$) we obtain the profile depicted in Figure 8. Therein, a local density maximum is found halfway between both surfaces.

4 Conclusions

A brief review was given illustrating that MC simulations are applicable to various chemical model systems. MC results are useful in comparison with both theoretical predictions and experimental measurement. MC simulations allow the study of both global and local properties of complex systems.

The Monte Carlo approach was applied to a system of two oppositely faced, interacting, self-assembled monolayers of amphiphile molecules using an off-lattice, good solvent model. Monolayers were modeled as grafted FR pearl-necklace chains with bond angle $\Theta = 90°$. Separated off-lattice monolayers show a behavior very similar to the one for lattice monolayers. In separated monolayers an increase in density results into increasing mean size properties. However, the opposite effect was observed while the density was increased by pressing two supported monolayers against each other.

The current off-lattice model was athermal. Future simulations will include a potential scheme for pearl-pearl and pearl-surface interactions to study the phase behavior and the forces between functionalized surfaces in contact.

Acknowledgments.

This work was supported by Grant No. SFB 285/B3 from the *Deutsche Forschungsgemeinschaft* in Bonn (Germany). The author would like to thank Uwe Reimer for his contribution to the section on self-assembly.

References

[1] N. G. Cooper, editor. *From Cardinals to Chaos.* Cambridge University Press, 32 East 57th Street, New York, NY 10022, USA, 1989.

[2] R. Eckhardt. *Stan Ulam, John von Neumann, and the Monte Carlo Method*, pages 131–141. In Cooper [1], 1989.

[3] N. Metropolis. *The Beginning of the Monte Carlo Method*, pages 125–130. In Cooper [1], 1989.

[4] W. H. Press; S. A. Teukolsky; W. T. Vetterling and B. P. Flannery, editors. *Numerical Recipes in C.* Cambridge University Press, Cambridge, 1992 (second edition).

[5] W. H. Press; S. A. Teukolsky; W. T. Vetterling and B. P. Flannery. *Random Numbers*, pages 274–328. In [4], 1992 (second edition).

[6] R. E. Crandall. *Projects in Scientific Computation.* Springer-Verlag, New York, 1994.

[7] R. E. Crandall. *Random numbers and Monte Carlo*, pages 42–50. In [6], 1994.

[8] P. Brémaud. *Markov Chains.* Springer-Verlag, New York, 1999.

[9] P. Brémaud. *Image Models*, pages 268–275. In [8], 1999.

[10] K. Binder, editor. *The Monte Carlo Method in Condensed Matter Physics.* Springer-Verlag, Berlin, 1992.

[11] M. P. Allen and D. J. Tildesley. *Computer Simulation in Chemical Physics.* Kluwer Academic Publishers, Dordrecht, 1993.

[12] J. W. Haefner. *Modeling Biological Systems.* Chapmann & Hall, New York, 1996.

[13] J. W. Haefner and T. O. Crist. Spatial model of movement and foraging in harvester ants (pogonomyrmex)(I): The roles of memory and communication. *J. theor. Biol.*, 166:299–313, 1994.

[14] D. Levesque and J. J. Weis. *Recent Progress in the Simulation of Classical Fluids*, pages 121–204. In Binder [10], 1992.

[15] M. P. Allen and D. J. Tildesley. *Computer Simulation of Liquids*. Clarendon Press, Oxford, reprinted 1996.

[16] A. Yethiraj and C. K. Hall. Monte Carlo simulations and integral equation theory for microscopic correlations in polymeric fluids. *J. Chem. Phys.*, 96:797–805, 1992.

[17] A. P. Malanoski and P. A. Monson. The high density equation of state and solid-fluid equilibrium in systems of freely jointed chains of tangent hard spheres. *J. Chem. Phys.*, 107:6899–6907, 1997.

[18] M. J. Vlot; H. E. A. Huitema; A. de Vooys and J. P. van der Eerden. Crystal structures of symmetric Lennard-Jones mixtures. *J. Chem. Phys.*, 107:4345–4349, 1997.

[19] M. J. Vlot; J. C. van Miltenburg; H. A. J. Oonk and J. P. van der Eerden. Phase diagrams of scalemic mixtures: A Monte Carlo simulation study. *J. Chem. Phys.*, 107:10102–101??, 1997.

[20] K. Binder, editor. *Monte Carlo and Molecular Dynamics Simulations in Polymer Science*. Oxford University Press, New York, 1995.

[21] L. Monnerie and U. W. Suter, editors. *Atomistic Modeling of Physical Properties*. Springer-Verlag, Berlin, 1994.

[22] A. Baumgärtner. *Simulations of Macromolecules*, pages 285–316. In Binder [10], 1992.

[23] R. E. Crandall. *Molecular biology*, pages 89–92. In [6], 1994.

[24] J. C. Gimel; T. Nicolai and D. Durand. 3D Monte Carlo simulations of diffusion limited cluster aggregation up to the sol-gel transition: Structure and kinetics. *J. Sol-Gel Sci. Technol.*, 15:129–136, 1999.

[25] A. Hasmy. Aerogelation process simulation by a cluster-cluster aggregation algorithm. *J. Sol-Gel Sci. Technol.*, 15:137–146, 1999.

[26] R. B. Pandey and Y. Liu. Simulations of sol-to-gel modeling: Effects of mobility, reversibility, and quality of solvent. *J. Sol-Gel Sci. Technol.*, 15:147–159, 1999.

[27] D. B. Butler and H. J. M. Hanley. Aggregation in quenched systems interacting through a short-range attractive, long-range repulsive potential. *J. Sol-Gel Sci. Technol.*, 15:161–166, 1999.

[28] R. Salazar; R. Toral and A. Chakrabarti. Phase behavior of binary fluid mixtures confined in a model aerogel. *J. Sol-Gel Sci. Technol.*, 15:175–181, 1999.

[29] D. Avnir, editor. *The Fractal Approach to Heterogeneous Chemistry*. John Wiley & Sons, Chichester, 1989.

[30] A. Bunde and S. Havlin, editors. *Fractals and Disordered Systems*. Springer-Verlag, Berlin, 1991.

[31] A. Aharony. *Fractal Growth*, pages 150–173. In Bunde and Havlin [30], 1991.

[32] P. Meakin. A historical introduction to computer models for fractal aggregates. *J. Sol-Gel Sci. Technol.*, 15:97–117, 1999.

[33] T. A. Witten Jr. and L. M. Sander. Diffusion-limited aggregation, a kinetic critical phenomenon. *Phys. Rev. Lett.*, 47:1400–1403, 1981.

[34] M. Kolb. Reversible diffusion-limited cluster aggregation. *J. Phys. A: Math. Gen.*, 19:L263–L268, 1986.

[35] M. Kolb. A Monte Carlo renormalisation group for aggregation processes. *J. Phys. A: Math. Gen.*, 20:L285–L289, 1987.

[36] J.-M. Debierre and L. Turban. Static and dynamic scaling for chain-chain aggregation in two dimensions. *J. Phys. A: Math. Gen.*, 20:L239–L244, 1987.

[37] C. Rioux M. Gauthier, M. Cossette and R. J. Slobodrian. Real and simulated fractal aggregates. *Chaos, Solitons & Fractals*, 3:687–694, 1993.

[38] F. Family and T. Vicsek, editors. *Dynamics of Fractal Surfaces*. World Scientific, Singapore, 1991.

[39] J.-F. Gouyet; M. Rosso and B. Sapoval. *Fractal Surfaces and Interfaces*, pages 228–261. In Bunde and Havlin [30], 1991.

[40] A.-L. Barabási and H. E. Stanley. *Fractal Concepts in Surface Growth*. Cambridge University Press, Cambridge, 1995.

[41] C. Uebing and R. Gomer. Diffusion of interacting lattice gases on homogeneous surfaces. *Ber. Bunsenges. Phys. Chem.*, 100:1138–1146, 1996.

[42] R. E. Crandall. *Quantum theory*, pages 102–106. In [6], 1994.

[43] Jr. J. W. Hammond; W. A. Lester and P. J. Reynolds. *Monte Carlo Methods in Ab Initio Quantum Chemistry*. World Scientific, Singapore, 1994.

[44] P. Langfelder; S. M. Rothstein and J. Vrbik. Diffusion quantum Monte Carlo calculation of nondifferential properties for atomic ground states. *J. Chem. Phys.*, 107:8525–8535, 1997.

[45] J. P. Hansen and I. R. McDonald. *Theory of Simple Liquids*. Academic Press., London, 1986.

[46] K. Lucas. *Applied Statistical Thermodynamics*. Springer-Verlag, Berlin, 1991.

[47] K. E. van Holde; W. C. Johnson and P. S. Ho. *Principles of Physical Biochemistry*. Prentice Hall, Upper Saddle River, New Jersey 07456, 1998.

[48] P. J. Flory. Statistical thermodynamics of liquid mixtures. *J. Am. Chem. Soc.*, 87:1833–1838, 1965.

[49] D. Frenkel and B. Smit. *Understanding Molecular Simulation*. Academic Press, San Diego, 1996.

[50] J. M. Haile. *Molecular Dynamics Simulation*. John Wiley & Sons, Inc., New York, 1992.

[51] M. N. Rosenbluth and A. W. Rosenbluth. Monte Carlo calculation of the average extension of molecular chains. *J. Chem. Phys.*, 23:356–359, 1955.

[52] F. T. Wall; L. A. Hiller and W. F. Atchison. Statistical computation of mean dimensions of macromolecules. II. *J. Chem. Phys.*, 23:913–921, 1955.

[53] F. T. Wall; R. J. Rubin and L. M. Isaacson. Improved statistical method for computing mean dimensions of polymer molecules. *J. Chem. Phys.*, 27:186–188, 1957.

[54] J. P. Downey. Static and dynamic scaling properties of single, self-avoiding polymer chains in two dimensions via the bond fluctuation method of Monte Carlo simulation. *Macromolecules*, 27:2929–2932, 1994.

[55] F. T. Wall; L. A. Hiller and W. F. Atchison. Statistical computation of mean dimensions of macromolecules. III. *J. Chem. Phys.*, 23:2314–2321, 1955.

[56] F. T. Wall; L. A. Hiller and W. F. Atchison. Statistical computation of mean dimensions of macromolecules. IV. *J. Chem. Phys.*, 26:1742–1749, 1957.

[57] F. T. Wall and J. J. Erpenbeck. New method for the statistical computation of polymer dimensions. *J. Chem. Phys.*, 30:634–637, 1959.

[58] F. T. Wall and J. J. Erpenbeck. Statistical computation of radii of gyration and mean internal dimensions of polymer molecules. *J. Chem. Phys.*, 30:637–640, 1959.

[59] Z. Alexandrowicz and Y. Accad. Monte Carlo of chains with excluded volume: Distribution of intersegmental distances. *J. Chem. Phys.*, 54:5338–5345, 1971.

[60] F. T. Wall and F. Mandel. Macromolecular dimensions obtained by an efficient Monte Carlo method without sample attrition. *J. Chem. Phys.*, 63:4592–4595, 1975.

[61] P. H. Verdier and W. H. Stockmayer. Monte Carlo calculations on the dynamics of polymers in dilute solution. *J. Chem. Phys.*, 36:227–235, 1962.

[62] P. H. Verdier. Monte Carlo studies of lattice-model polymer chains. II. end-to-end length. *J. Chem. Phys.*, 45:2122–2128, 1966.

[63] H. J. Hilhorst and J. M. Deutch. Analysis of Monte Carlo results on the kinetics of lattice polymer chains with excluded volume. *J. Chem. Phys.*, 63:5153–5161, 1975.

[64] M. Lax and C. Brender. Monte Carlo study of lattice polymer dynamics. *J. Chem. Phys.*, 67:1785–1787, 1977.

[65] Z.-Y. Chen and P. Weakliem. Numerical study of hydrodynamic radii of polymer chains in θ solvent. *Macromolecules*, 23:280–283, 1990.

[66] H. Meirovitch. Efficient dynamical Monte Carlo method for dense polymer systems. *Macromolecules*, 17:2038–2044, 1984.

[67] K. Binder. *Introduction: General Aspects of Computer Simulation Techniques and Their Application in Polymer Physics*, pages 3–46. In [20], 1995.

[68] R. H. Boyd and P. J. Philipps. *The statistical behavior of conformationally disordered chains*, pages 188–227. In [84], 1996.

[69] M. P. Tarazona and E. Saiz. Models for models: An introduction to polymer models employing simple analogies. *J. Chem. Educ.*, 75:1425–1429, 1998.

[70] G. H. Weiss. *Aspects and Applications of the Random Walk.* North-Holland Elsevier Science B. V., Amsterdan, The Netherlands, 1994.

[71] K. Binder and D. W. Heermann. *Monte Carlo Simulation in Statistical Physics*. Springer-Verlag, Berlin, 1992.

[72] P. J. Flory. *Statistical Mechanics of Chain Molecules*. Hanser Publishers, Munich, 1989.

[73] A. D. Sokal. *Monte Carlo Methods for the Self-Avoiding Walk*, pages 47–124. In Binder [20], 1995.

[74] O. F. Olaj; T. Petrik and G. Zifferer. Concentration dependence of static chain properties, 1 Monte Carlo simulations in a cubic lattice. *Macromol. Theory Simul.*, 6:1277–1302, 1997.

[75] A Drefahl; O. Seidel and H.-J. Mögel. Nanosystem similarity: Modeling and comparison of amphiphilic monolayers adsorbed on nanorough surfaces. *J. Chem. Inf. Comput. Sci.*, 38:1223–1231, 1998.

[76] S. Hemmer and P. C. Hemmer. An average self-avoiding random walk on the square lattice lasts 71 steps. *J. Chem. Phys.*, 81:584–585, 1984.

[77] W. Kuhn. Über die Gestalt fadenförmiger Moleküle in Lösung. *Kolloid-Z.*, 68:2–15, 1934.

[78] J. Baschnagel; K. Qin; W. Paul and K. Binder. Monte carlo simulation of models for single polyethylene coils. *Macromolecules*, 25:3117–3124, 1992.

[79] L. R. Dodd and D. N. Theodorou. *A Critical Evaluation of Novel Algorithms for the Off-Lattice Monte Carlo Simulation of Condensed Polymer Phases*, pages 283–318. In Monnerie and Suter [21], 1994.

[80] P.-G. de Gennes. *Scaling Concepts in Polymer Physics*. Cornell Unversity Press, Ithaca and London, 1979.

[81] K. Kremer. *Computer Simulation of Polymers*, pages 397–459. In [11], 1993.

[82] O. F. Olaj; T. Petrik and G. Zifferer. Concentration dependence of static chain properties 2, off-lattice Monte Carlo simulations. *J. Chem. Phys.*, 23:10214–10224, 1997.

[83] A. Baumgärtner. Statics and dynamics of the freely jointed polymer chain with lennard-jones interaction. *J. Chem. Phys.*, 72:871–879, 1980.

[84] R. H. Boyd and P. J. Philipps. *The Science of Polymer Molecules*. Cambridge University Press, Cambridge, 1996.

[85] G. R. Strobl. *The Physics of Polymers*. Springer-Verlag, Berlin, 1996.

[86] K. Binder. *Computer Simulations of Tethered Chains*, pages 476–578. In [20], 1995.

[87] J. E. G. Lipson; S. G. Whittington; M. K. Wilkinson; J. L. Martin and D. S. Gaunt. A lattice model of uniform star polymers. *J. Phys. A: Math. Gen.*, 18:L469–L473, 1985.

[88] I. Romantsova and Y. Taran. Computer simulation of the dynamics of branched polymers. *Makromol. Chem.*, 191:2423–2433, 1990.

[89] S.-J. Su; M. S. Denny and J. Kovac. Computer simulation of the dynamics of shape fluctuations in uniform star polymers. *Macromolecules*, 24:917–923, 1991.

[90] S.-J. Su and J. Kovac. Concentration dependence of shape fluctuations of uniform star polymers. *J. Phys. Chem*, 96:3931–3934, 1992.

[91] C. H. Vlahos; A. Horta; N. Hadjichristidis and J. J. Freire. Monte carlo calculations of $(a_x b_{f-x})$ miktoarm star copolymers. *Macromolecules*, 28:1500–1505, 1995.

[92] K. Ohno; K. Shida; M. Kimura and Y. Kawazoe. Monte Carlo study of the second virial coefficient of star polymers in a good solvent. *Macromolecules*, 29:2269–2274, 1996.

[93] A. M. Rubio and J. J. Freire. Monte Carlo calculation of second virial coefficients for linear and star chains in a good solvent. *Macromolecules*, 29:6946–6951, 1996.

[94] Z. Y. Chen and S.-M. Cui. Monte Carlo simulations of star-burst dendrimers. *Macromolecules*, 29:7943–7952, 1996.

[95] Y. Roualt and O. V. Borisov. Com-branched polymers: Monte Carlo simulation and scaling. *Macromolecules*, 29:2605–2611, 1996.

[96] J. J. Freire; R. Prats; J. Pla and J. G. de la Torre. Hydrodynamic properties of flexible branched chains. Monte Carlo nonpreaveraged calculations for stars and preaveraged results for combs. *Macromolecules*, 17:1815–1821, 1984.

[97] J. M. J. Fréchet. Functional polymers and dendrimers: Reactivity, molecular architecture, and interfacial energy. *Science*, 263:1710–1715, 1994.

[98] H. S. Chan and K. A. Dill. Sequence space soup of proteins and copolymers. *J. Chem. Phys.*, 95:3775–3787, 1991.

[99] A. Šali; E. Shakhnovich and M. Karplus. How does a protein fold? *Nature*, 369:248–251, 1994.

[100] N. L. Nunes; K. Chen and J. S. Hutchinson. Flexible lattice model to study protein folding. *J. Phys. Chem.*, 100:10443–10449, 1996.

[101] A. R. Dinner and M. Karplus. The thermodynamics and kinetics of protein folding: A lattice model analysis of multiple pathways with intermediates. *J. Phys. Chem.*, 103:7976–7994, 1999.

[102] H. S. Chan and K. A. Dill. Intrachain loops in polymers: Effects of excluded volume. *J. Chem. Phys.*, 90:492–509, 1989.

[103] H. S. Chan and K. A. Dill. The effect of internal constraints on the configurations of chain molecules. *J. Chem. Phys.*, 92:3118–3235, 1990.

[104] H. S. Chan; M. R. Wattenbarger; D. F. Evans; V. A. Bloomfield and K. A. Dill. Enhanced structure in polymers at interfaces. *J. Chem. Phys.*, 94:8542–8557, 1991.

[105] D. Gersappe; W. Li and A. C. Balazs. Computational studies of protein adsorption at bilayer interfaces. *J. Chem. Phys.*, 99:7209–7213, 1993.

[106] K. E. van Holde; W. C. Johnson and P. S. Ho. *Nonregular Structures*, pages 179–189. In [47], 1998.

[107] H. S. Chan and K. A. Dill. 'sequence space soup' of proteins and copolymers. *J. Chem. Phys.*, 95:3775–3787, 1991.

[108] A. Irbäck; C. Petersen; F. Potthast and O. Sommelius. Local interactions and protein folding: A three-dimensional off-lattice approach. *J. Chem. Phys.*, 107:273–282, 1997.

[109] P.-G. de Gennes. *Polymer Solutions in Good Solvents*, pages 69–97. In [80], 1979.

[110] P. J. Flory. *Principles of Polymer Chemistry*. Cornell University Press, Ithaca, New York, 1953.

[111] K. Binder. *Monte Carlo Studies of Polymer Blends and Block Copolymer Thermodynamics*, pages 356–432. In [20], 1995.

[112] A. Sariban and K. Binder. Critical properties of the Flory-Huggins lattice model of polymer mixtures. *J. Chem. Phys.*, 86:5859–5873, 1987.

[113] I. Szleifer and A. Z. Panagiotopoulos. Chain length and density dependence of the chemical potential of lattice polymers. *J. Chem. Phys.*, 97:6666–6673, 1992.

[114] M. Müller and K. Binder. Computer simulation of asymmetric polymer mixtures. *Macromolecules*, 28:1825–1834, 1995.

[115] W. Bruns. The second osmotic virial coefficient of polymer solutions. *Macromolecules*, 29:2641–2643, 1996.

[116] A. Yethiraj; K. G. Honnell and C. K. Hall. Monte Carlo calculation of the osmotic second virial coefficient of off-lattice athermal polymers. *Macromolecules*, 25:3979–3983, 1992.

[117] P. Cifra; E. Nies and J. Broersma. Equation of state and miscibility behavior of compressible binary lattice polymers. a Monte Carlo study and comparison with partition function theories. *Macromolecules*, 29:6634–6644, 1996.

[118] G. J. A. Ypma; P. Cifra; E. Nies and A. R. D. Bergen. Interfacial behavior of compressible polymer blends. Monte Carlo simulation and the lattice fluid theory. *Macromolecules*, 29:1252–1259, 1996.

[119] O. F. Olaj; T. Petrik and G. Zifferer. Monte Carlo simulation of symmeteric polymer blends. II. chain properties in interface regions. *J. Chem. Phys.*, 108:8226–8234, 1998.

[120] P. M. Holland and D. N. Rubingh, editors. *Mixed Surfactant Systems*. American Chemical Society, Washington, DC, 1992.

[121] I. D. Robb, editor. *Specialist Surfactants*. Chapman & Hall, London, 1997.

[122] B. Jönsson; B. Lindman; K. Holmberg and B. Kronberg, editors. *Surfactants and Polymers in Aqueous Solution*. John Wiley & Sons, Chichester, 1998.

[123] J. van Stam; S. Depaemelaere and F. C. De Schryver. Micellar aggregation numbers - a fluorescence study. *J. Chem. Educ.*, 75:93–98, 1998.

[124] P. D. T. Huibers; V. S. Lobanov; A. R. Katritzky; D. O. Shah and M. Karelson. Prediction of critical micelle concentration using a quantitative structuture-property relationship approach. 1. nonionic surfactants. *Langmuir*, 12:1462–1470, 1996.

[125] P. D. T. Huibers; V. S. Lobanov; A. R. Katritzky; D. O. Shah and M. Karelson. Prediction of critical micelle concentration using a quantitative structuture-property relationship approach. 1. anionic surfactants. *J. Colloid. Interface Sci.*, 115:113–120, 1997.

[126] J. N. Israelachvili; D. J. Mitchell and B. W. Nimham. Hydrocarbon amphiphiles into micelles and bilayers. *J. Chem. Soc., Faraday. Trans. II*, 72:1525–1568, 1976.

[127] B. Owenson and L. R. Pratt. Molecular statistical thermodynamics of model micellar aggregates. *J. Phys. Chem.*, 88:2905–2915, 1984.

[128] C. M. Care. Cluster size distribution in a Monte Carlo simulation of the micellar phase of an amphiphile and solvent mixture. *J. Chem. Soc., Faraday Trans. 1*, 83:2905–2912, 1987.

[129] K. Rodrigues and W. L. Mattice. Segmental distribution functions for a micelle comprised of small symmetric diblock copolymers (short chain amphiphiles). *J. Chem. Phys.*, 95:5341–5347, 1991.

[130] R. G. Larson. Monte Carlo simulation of microstructural transitions in surfactant systems. *J. Chem. Phys.*, 96:7904–7918, 1992.

[131] C. M. Wijmans and P. Linse. Modeling of nonionic micelles. *Langmuir*, 11:3748–3756, 1995.

[132] P. H. Nelson; G. C. Rutledge and T. A. Hatton. On the size and shape of self-assembled micelles. *J. Chem. Phys.*, 107:10777–10781, 1997.

[133] L. R. Rodríguez-Guadarama; S. K. Talsania; K. K. Mohanty and R. Rajagopalan. Thermodynamics of aggregation of amphiphiles in solution from lattice Monte C arlo simulations. *Langmuir*, 15:437–446, 1999.

[134] M. A. Floriano and E. Caponetti. Micellization in model surfactant systems. *Langmuir*, 15:3143–3151, 1999.

[135] B. Smit. *Computer Simulation of Surfactants*, pages 461–472. In [11], 1993.

[136] A. Milchev and K. Binder. Formation of surface micelles from adsorbed asymmetric block copolymers: A Monte Carlo study. *Langmuir*, 15:3232–3241, 1999.

[137] Y. Zhan and W. L. Mattice. Self-assembly and adsorption of diblock copolymers from selective solvents 1. self-assembly. *Macromolecules*, 27:677–682, 1994.

[138] S. K. Talsania; Y. Wang; R. Rajagopalan and K. K. Mohanty. Monte Carlo simulations for micellar encapsulation. *J. Colloid Interface Sci.*, 190:92–103, 1997.

[139] A. Bhattacharya; S. D. Mahanti and A. Chakrabarti. Self-assembly of neutral and ionic surfactants: An off-lattice Monte Carlo approach. *J. Chem. Phys.*, 108:10281–10293, 1998.

[140] D. Brindle and C. M. Care. Phase diagram for the lattice model of amphiphile and solvent mixtures by Monte Carlo simulation. *J. Chem. Soc. Faraday Trans.*, 88:2163–2166, 1992.

[141] A. T. Bernardes. Computer simulations of spontaneous vesicle formation. *Langmuir*, 12:5763–5767, 1996.

[142] A Drefahl; M. Wahab; P. Schiller and H.-J. Mögel. A Monte Carlo study of bilayer formation in a lattice model. *Thin Solid Films*, 327-329:846–849, 1998.

[143] M. Wahab. *Simulation, Berechnung und Visualisierung von Modellen ausgewählter biochemisch relevanter Strukturen*. PhD thesis, Martin-Luther University Halle-Wittenberg, Germany, 1998.

[144] U. Reimer; O. Seidel; A. Drefahl and H.-J. Mögel. Monte-Carlo-Simulation selbstorganisierter Tensidschichten an Festkörperoberflächen. *Freiberger Forschungshefte*, A 841 Grundstoff-Verfahrenstechnik:253–266, 1998.

[145] G. M. Foo and R. B. Pandey. Electro-deposition of polymer chains on an adsorbing wall: Density profiles and wall coverage. *J. Chem. Phys.*, 107:10260–10267, 1997.

[146] R. Zajac and A. Chakrabarti. Statics and dynamics of homopolymer adsorption and desorption: A Monte Carlo study. *J. Chem. Phys.*, 104:2418–2437, 1996.

[147] R. B. Pandey; A. Milchev and K. Binder. Semidilute and concentrated polymer solutions near attractive walls: Dynamic Monte Carlo simulation of density and pressure profiles of a coarse-grained model. *Macromolecules*, 30:1194–1204, 1997.

[148] T. C. Clancy and S. E. Webber. Controlling adsorption of polymer-modified surfaces. *Macromolecules*, 30:1340–1346, 1997.

[149] A. K. Chakroborty and D. Bratko. A simple theory and Monte Carlo simulations for recognition between random heteropolymers and disordered surfaces. *J. Chem. Phys.*, 108:1676–1682, 1998.

[150] C. Zuppa; M. Ciacera and G. Zgrablich. Cooperative sequential adsorption of k-mers on heterogeneous substrates. *Langmuir*, 15:5984–5989, 1999.

[151] A. J. Ramirez-Pastor; V. D. Pereyra and J. L. Riccardo. Statistical thermodynamics of linear adsorbates in low dimensions: Application to adsorption on heterogeneous surfaces. *Langmuir*, 15:5707–5712, 1999.

[152] A. Georgallas and D. A. Pink. Phase transitions in monolayers of saturated lipids. exact results and Monte Carlo simulations. *Jornal of Colloid and Interface Science*, 89:107–116, 1982.

[153] Z.-Y. Chen; J. Talbot; W. M. Gelbart and A. Ben-Shaul. Phase-transitions in systems of grafted rods. *Pys. Rev. Lett.*, 61:1376–1379, 1988.

[154] N. Collazo and S. A. Rice. Long-chain amphiphile monolayers on an anisotropic substrate: A computer simulation study. *Langmuir*, 7:3144–3153, 1991.

[155] D. Kramer; A. Ben-Shaul; Z.-Y. Chen and W. M. Gelbart. Monte Carlo and mean-field studies of successive phase transitions in rod monolayers. *J. Chem. Phys.*, 96:2236–2252, 1992.

[156] D. Kramer and A. Ben-Shaul. Phase transitions in a monolayer of interconverting squares. *Physica A*, 195:12–30, 1993.

[157] J. Harris and S. A. Rice. A lattice model of a supported monolayer of amphiphile molecules: Monte Carlo simulation. *J. Chem. Phys.*, 88:1298–1306, 1992.

[158] A. Chakrabarti and R. Toral. Density profile of terminally anchored polymer chains: A Monte Carlo study. *Macromolecules*, 23:2016–2021, 1990.

[159] P.-Y. Lai and K. Binder. Structure and dynamics of grafted polymer layers: A Monte Carlo simulation. *J. Chem. Phys.*, 95:9288–9299, 1991.

[160] P.-Y. Lai and K. Binder. Structure and dynamics of polymer brushes near the θ point: A Monte Carlo simulation. *J. Chem. Phys.*, 97:586–595, 1992.

[161] M. Milik; A Kolinski and J. Skolnick. Monte Carlo dynamics of a dense system of chain molecules constrained to lie near an interface. a simplified membrane model. *J. Chem. Phys.*, 93:4440–4446, 1990.

[162] M. Scheringer; R. Hilfer and K. Binder. Orientational ordering in lipid monolayers: A two-dimensional model of rigid rods grafted onto a lattice. *J. Phys. Chem*, 96:2269–2277, 1992.

[163] Y. K. Levine; A. Kolinski and J. Skolnick. A lattice dynamics study of a Langmuir monolayer of monounsaturated fatty acids. *J. Chem. Phys.*, 98:7581–7587, 1993.

[164] P.-Y. Lai. Grafted polymer layers with chain exchange: A Monte Carlo simulation. *J. Chem. Phys.*, 98:669–673, 1993.

[165] H. Stettin; R. Friedemann and H.-J. Mögel. Monte Carlo simulations of supported monolayers of amphiphilic molecules. *Ber. Bunsenges. Phys. Chem.*, 97:44–48, 1993.

[166] H. Stettin and H.-J. Mögel. Amphiphilic molecules with a structured head on a water surface: a Monte Carlo simulation. *Progr. Colloid. Polym. Sci.*, 97:27–30, 1994.

[167] H. Stettin and H.-J. Mögel. Branched amphiphilic molecules on a water surface: a Monte Carlo simulation. *Progr. Colloid. Polym. Sci.*, 97:31–34, 1994.

[168] H. Stettin; M. Wahab; P. Schiller; and H.-J. Mögel. Self-assembling of chain molecules in low dimension: a Monte Carlo study. *Macromol. Theory Simul.*, 4:1015–1037, 1995.

[169] H. Stettin; H.-J. Mögel and C. M. Care. Monolayer model simulations of mixtures of amphiphilic molecules. *Ber. Bunsenges. Phys. Chem.*, 100:20–26, 1996.

[170] S. Balasubramanian; M. L. Klein and J. I. Siepmann. Monte Carlo investigations of hexadecane films on a metal substrate. *J. Chem. Phys.*, 103:3184–3195, 1995.

[171] F. M. Haas; R. Hilfer and K. Binder. Layers of semiflexible chain molecules endgrafted at interfaces: An off-lattice Monte Carlo simulation. *J. Chem. Phys.*, 102:2960–2969, 1995.

[172] A. Milchev; V. Yamakov and K. Binder. Escape transition of a polymer chain: Phenomenological theory and Monte Carlo simulations. *Phys. Chem. Chem. Phys.*, 1:2083–2091, 1999.

[173] A Drefahl; O. Seidel and H.-J. Mögel. Monolayer properties of amphiphilic molecules supported on nano-rough surfaces: a Monte Carlo study. *Thin Solid Films*, 327-329:850–853, 1998.

[174] F. M. Haas; P.-Y. Lai and K. Binder. Linear chain surfactants at a planar interface: a comparative Monte Carlo study of several lattice models. *Makromol. Chem. Theory Simul.*, 2:889–899, 1993.

[175] J. J. de Pablo; M. Laso and U. W. Suter. Simulation of polyethylene above and below the melting point. *J. Chem. Phys.*, 96:2395–2403, 1992.

[176] S. Misra and W. L. Mattice. Telechelic polymers between two impenetrable adsorbing surfaces. *Macromolecules*, 27:2058–22065, 1994.